New Limits on Intrinsic Charm in the Nucleon from Global Analysis of Parton Distributions

P. Jimenez-Delgado,[1] T. J. Hobbs,[2,3] J. T. Londergan,[2] and W. Melnitchouk[1]
[1]Jefferson Lab, 12000 Jefferson Avenue, Newport News, Virginia 23606, USA
[2]Department of Physics and Center for Exploration of Energy and Matter, Indiana University, Bloomington, Indiana 47405, USA
[3]Department of Physics, University of Washington, Seattle, Washington 98195, USA
(Received 7 August 2014; revised manuscript received 20 January 2015; published 27 February 2015)

We present a new global QCD analysis of parton distribution functions, allowing for possible intrinsic charm (IC) contributions in the nucleon inspired by light-front models. The analysis makes use of the full range of available high-energy scattering data for $Q^2 \gtrsim 1$ GeV^2 and $W^2 \gtrsim 3.5$ GeV^2, including fixed-target proton and deuteron cross sections at lower energies that were excluded in previous global analyses. The expanded data set places more stringent constraints on the momentum carried by IC, with $\langle x \rangle_{\rm IC}$ at most 0.5% (corresponding to an IC normalization of ~1%) at the 4σ level for $\Delta\chi^2 = 1$. We also critically assess the impact of older EMC measurements of F_2^c at large x, which favor a nonzero IC, but with very large χ^2 values.

DOI: 10.1103/PhysRevLett.114.082002 PACS numbers: 14.65.Dw, 13.60.Hb, 12.38.-t

There has been considerable interest recently in the nature of Fock states of the proton wave function involving five or more quarks, such as $|uudq\bar{q}\rangle$, where $q = u, d, s$ or c [1–6]. This has arisen partly from attempts to understand flavor asymmetries observed in the nucleon sea, such as $\bar{d} > \bar{u}$ [7,8] and $s \neq \bar{s}$ [9], which clearly point to a nonperturbative origin. In addition, there has been a long-standing debate about the existence of intrinsic charm (IC) quarks in the proton, associated with the $|uudc\bar{c}\rangle$ component of the proton wave function.

Aside from the intrinsic interest in the role of nonperturbative dynamics in the structure of the nucleon sea, the leptoproduction of charm quarks is also important in providing information on the gluon distribution in the nucleon. A significant IC component in the nucleon wave function could also influence observables measured at the LHC, either directly through enhanced cross sections at large x, or indirectly via the momentum sum rule leading to a decreased momentum fraction carried by gluons.

Following early indications from measurements of charm production in pp scattering of an anomalous excess of D mesons at large values of Feynman x_F (see [10] and references therein), the proposal was made that the observed enhancement could be accounted for with the addition of intrinsic $c\bar{c}$ pairs in the nucleon that were not generated through perturbative gluon radiation [11]. Neglecting quark transverse momentum and assuming a charm mass much greater than other mass scales, Brodsky, Hoyer, Peterson, and Sakai (BHPS) [11] derived an analytic approximation to the IC distribution that, unlike the perturbatively generated charm, was peaked at relatively large parton momentum fractions x.

A number of experimental and theoretical studies have since sought to elucidate this issue, although the evidence has been somewhat inconclusive. Measurements of the charm structure function F_2^c by the European Muon Collaboration (EMC) [12] provided tantalizing evidence for an enhancement at large x; however, more recent experiments at HERA [13] at small x found significant tension with the EMC data in regions of overlapping kinematics.

Early theoretical analyses of the EMC charm data indicated an IC component with normalization $N_{\rm IC} \equiv \int_0^1 dx c(x) \sim 1\%$, although later, more sophisticated treatments incorporating the photon-gluon fusion (PGF) process, as well as quark and target mass corrections, argued for smaller IC, ~0.3% [14]. A subsequent study by Harris, Smith, and Vogt [15] which included $\mathcal{O}(\alpha_s)$ corrections to the hard scattering cross section, obtained a best fit to the highest-energy EMC data with $N_{\rm IC} = (0.86 \pm 0.60)\%$. A follow-up analysis by Steffens *et al.* [16] employed a hybrid scheme to interpolate between massless evolution at large Q^2 and PGF at low Q^2, using the BHPS IC model and a model based on fluctuations of the nucleon to charmed baryon and D meson states [17–19]. While it was difficult to fit the data simultaneously in terms of a single IC framework, Steffens *et al.* found a slight preference for IC in the meson-baryon model at a level of $N_{\rm IC} \approx 0.4\%$.

To place the study of IC on a more robust statistical footing, Pumplin *et al.* [20] used the framework of the CTEQ global fit [21] to parton distribution functions (PDFs) to determine the level of IC that could be accommodated by the high-energy data. Comparing the BHPS model, a $p \to \Lambda_c^+ \bar{D}^0$ fluctuation model with scalar couplings, and a sealike ansatz in which the charm distribution is proportional to the $\bar{u}$ and $\bar{d}$ PDFs, the analysis found an allowed range of IC from zero to a level 2–3 times larger than earlier estimates [20].

An updated NNLO fit by Dulat *et al.* [22], based on the more recent CT10 global analysis [23] and the BHPS and

sealike IC models, found the momentum fraction carried by intrinsic charm quarks,

$$\langle x\rangle_{\rm IC} \equiv \int_0^1 dx x[c(x)+\bar{c}(x)], \quad (1)$$

to be $\lesssim 2.5\%$ for the BHPS distribution at the 90% confidence level. Note that for the BHPS distribution with a 1% normalization, the corresponding momentum fraction is $\langle x\rangle_{\rm IC} = 0.57\%$. The Dulat *et al.* analysis therefore suggests that the existing data may tolerate rather significant momentum carried by IC.

In this Letter, we revisit the question of the magnitude of IC allowed by the world's F_2^c and other high-energy data, by performing a new global QCD analysis, along the lines of the recent JR14 fit [24]. Unlike previous global analyses [20,22] that placed more stringent cuts on the data ($Q^2 \gtrsim 4$ GeV^2 and $W^2 \gtrsim 12$ GeV^2), excluding, for instance, all fixed target measurements from SLAC [25], we include all available data sets with $Q^2 \geq 1$ GeV^2 and $W^2 \geq 3.5$ GeV^2. Since most IC models predict this effect to be most prominent at large values of x, excluding the largest-x data may seriously reduce the sensitivity of the global fit to any IC that may be present. In addition, we assess the consistency of the EMC F_2^c data [12], which have often been cited as providing the strongest evidence for IC in high-energy processes.

Of course, inclusion of lower-Q^2 data requires careful treatment of finite-Q^2 and nuclear corrections at intermediate and large x. Following Refs. [24,26–28], we account for target mass corrections explicitly, using the moment space results for F_2 and F_L from Ref. [29], and allow for phenomenological $1/Q^2$ higher twist contributions. For nuclear smearing and nucleon off-shell corrections in the deuteron, we adopt the method used in the CJ global analysis [27,28], while for data on heavier nuclei the nuclear PDFs from Ref. [30] are employed. Also, whenever possible, we fit the original cross section data rather than structure functions derived using an assumed longitudinal to transverse cross section ratio. (Further details about the QCD analysis can be found in Ref. [24].)

For the QCD analysis we use the framework of the JR14 global fit [24], in which the F_2 structure function

$$F_2 = F_2^{\rm light} + F_2^{\rm heavy} \quad (2)$$

is decomposed into light (u, d, s) and heavy (c, b) quark contributions. The charm structure function is further decomposed into perturbative ($F_2^{c\bar{c}}$) and nonperturbative ($F_2^{\rm IC}$) components,

$$F_2^c = F_2^{c\bar{c}} + F_2^{\rm IC}. \quad (3)$$

The perturbative part is computed in the fixed-flavor number scheme (FFNS) from the PGF process [31],

$$F_2^{c\bar{c}}(x,Q^2,m_c^2) = \frac{Q^2\alpha_s}{4\pi^2 m_c^2}\sum_i \int \frac{dz}{z}\hat{\sigma}_i(\eta,\xi) f_i\left(\frac{x}{z},\mu\right), \quad (4)$$

where $\hat{\sigma}_i$ is the hard scattering cross section for the production of a $c\bar{c}$ pair from a parton of flavor i ($i = u, d, s$ or g), and f_i is the corresponding parton distribution, both calculated to NLO [$\mathcal{O}(\alpha_s)$] accuracy. The partonic cross section $\hat{\sigma}_i$ is evaluated as a function of the scaling variables $\xi = Q^2/m_c^2$ and $\eta = Q^2(1-z)/(4m_c^2 z) - 1$, and the PDF is computed at the factorization scale $\mu^2 = 4m_c^2 + Q^2$. The analysis therefore fully takes into account the kinematical corrections arising from quark and target mass effects. In the FFNS the charm mass does not enter the evolution equations directly (only indirectly through the running of α_s). For the running mass of the charm quark we take $m_c(m_c) = 1.3$ GeV at the charm scale in the $\overline{\rm MS}$ scheme; reasonable variations in the value of m_c have only a slight impact on the results and do not affect our conclusions.

For the nonperturbative charm contributions to F_2^c, we consider several models from recent IC analyses, including variants of the meson-baryon fluctuation model used to describe charmed baryon production in hadronic collisions [10], and the BHPS five-quark model [11]. The meson-baryon model of Ref. [10] includes virtual meson-baryon configurations with pseudoscalar $\bar{D}$ and vector $\bar{D}^*$ mesons of mass up to ≈ 2 GeV, and spin-1/2 (Λ_c, Σ_c) and spin-3/2 (Σ_c^*) charm baryons. In contrast, the meson-baryon model of Pumplin [19] generated IC distributions from the fluctuation of the nucleon to a scalar $\bar{D}\Lambda_c$ state. To regulate the short-distance behavior of the hadronic loop integrals, a Gaussian form factor was introduced to dampen the high-momentum components of the hadronic light-cone distributions, with the cutoff parameter fit to reproduce the inclusive charmed baryon and meson production in NN collisions [10].

The IC distributions in the nucleon were then obtained by convoluting the charmed meson and baryon distributions with the corresponding PDFs in the charmed hadrons. In the present analysis we fix the shapes of the IC distributions computed in Ref. [10] by the respective best fit cutoff parameters, but allow the overall normalization to vary. Provided the variation of the cutoffs is not dramatic, the effect on the shape of the IC distribution is minor. Note that the meson-baryon fluctuation model naturally accommodates asymmetric c and $\bar{c}$ distributions as a function of x [17]. Finally, from the IC distribution in a given model, the IC contribution to the charm structure function is computed using the framework of Hoffman and Moore [14] to $\mathcal{O}(\alpha_s)$.

The results of the global analysis are summarized in Fig. 1, where the total χ^2 values for each of the 26 data sets used in the fit are shown (relative to the value for no IC, χ_0^2) as a function of the momentum fraction carried by IC quarks. The total χ^2 has its minimum for zero IC, and rises rapidly with increasing $\langle x\rangle_{\rm IC}$. The largest contributions to

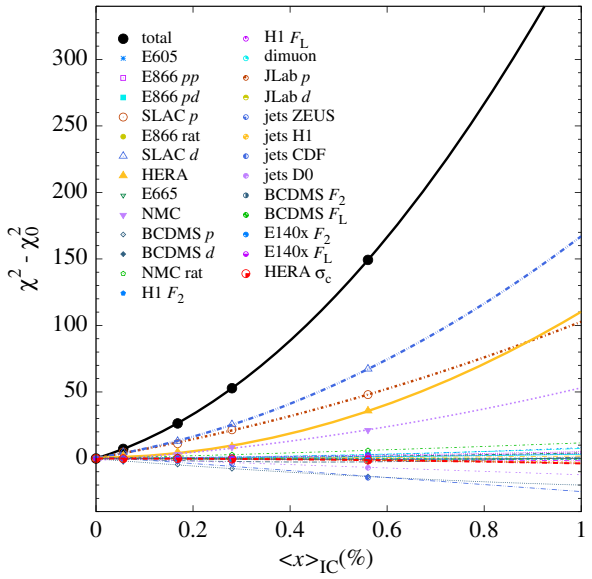

FIG. 1 (color online). Contributions to the total χ^2 (black circles), relative to the value χ^2_0 for no IC, of various data sets as a function of the momentum fraction $\langle x\rangle_{\rm IC}$ carried by IC quarks (in percent). The largest contributions to the total χ^2 are from the SLAC inclusive deuteron (blue triangles) and proton (brown circles) structure functions, HERA F_2^c (orange triangles) and NMC F_2 (violet triangles) data. The EMC F_2^c data are not included in this fit.

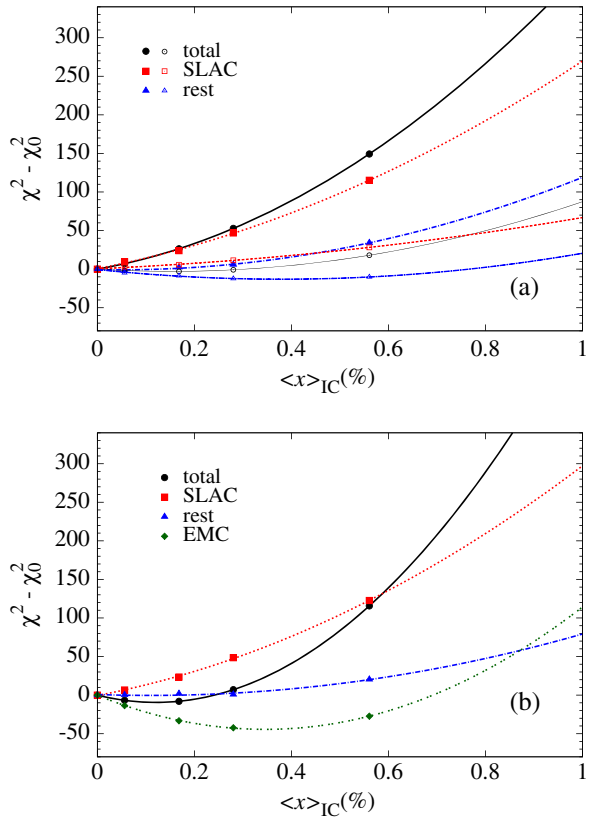

FIG. 2 (color online). Contributions of various data sets to the total χ^2, relative to χ^2_0, as a function of $\langle x\rangle_{\rm IC}$ (in percent) for (a) the standard data set, and (b) including the EMC F_2^c data. In (a), the upper curves (filled symbols) represent the standard fit, while the lower curves (open symbols) include a threshold suppression factor [33].

χ^2 arise from the SLAC deep-inelastic proton and deuteron structure functions [25], with smaller contributions from HERA charm production at low x [13], and NMC proton and deuteron cross sections in the medium-x region [32]. All other data sets have little or no sensitivity to IC, as evidenced by the rather shallow χ^2 profiles. The total χ^2 for the global fit gives $\chi^2/N_{\rm dat} = 1.25$ for $N_{\rm dat} = 4296$ data points.

Because of the more restrictive Q^2 and W^2 cuts employed in previous global IC studies [20,22], which were tuned more to collider data, lower energy fixed-target data such as from SLAC were excluded from the fits. This produced rather weak limits on the IC momentum fraction, $\langle x\rangle_{\rm IC} \lesssim 2\%$–$3\%$. Including the full data set, we find a much more stringent constraint on the momentum carried by IC, with $\langle x\rangle_{\rm IC} < 0.1\%$ at the 5σ level. The rest of the χ^2 profile allows slightly larger IC values, as illustrated in Fig. 2(a), with $\langle x\rangle_{\rm IC} < 0.1\%$ at the 1σ level.

Note that a significant portion of the SLAC data (360 points from a total of 1021) lie below the partonic charm threshold, $W^2 < 4m_c^2$, so that these data do not provide direct constraints on IC. However, through Q^2 evolution the stronger constraints on the light-quark PDFs at high x from the low-W region allow important limitations on the magnitude of the IC to be obtained from the global fit to the expanded data set. In fact, the partonic threshold is lower than the physical threshold at which charmed hadrons can be produced, which in DIS would correspond to $W^2 > W^2_{\rm thr} \approx 16\ {\rm GeV}^2$. Even above this value there are still 157 data points in the SLAC p and d data sets.

To take into account the mismatch between the partonic and hadronic charm thresholds, various prescriptions have been adopted in the literature. The MSTW analysis [34] employed a "modified threshold" approach with an effective charm quark mass $m_c(1 + \Lambda^2/m_c^2)$ in the threshold dependent parts of coefficient functions, where Λ is a "binding energy" parameter. An alternative prescription [33] advocates a phase space factor $\theta(W^2 - W^2_{\rm thr})(1 - W^2_{\rm thr}/W^2)$ weighting F_2^c in Eq. (3) to suppress charm contributions near threshold. The fits with the hadron suppression factor, illustrated in Fig. 2(a), show a generally shallower χ^2 profile, with $\langle x\rangle_{\rm IC}$ at most $\approx 0.5\%$ at the 4σ level. The minimum χ^2 in this case occurs at $\langle x\rangle_{\rm IC} = (0.15 \pm 0.09)\%$ for the full data set.

The differences between our analysis without the SLAC data and those in Refs. [20,22] are partly explained by the different tolerance criteria used: in our fits the PDF errors refer to variations of $\Delta\chi^2 = 1$ around the minimum [24,35], whereas the previous analyses [20,22] assumed a tolerance of $\Delta\chi^2 = 100$. There is no unique criterion for selecting the

correct $\Delta\chi^2$ interval, and we use the traditional $\Delta\chi^2 = 1$ choice based on statistical considerations alone. Choosing $\Delta\chi^2 = 100$ would inflate the uncertainty and accommodate $\langle x\rangle_{\rm IC} \approx 1\%$ at the 1σ level, which is comparable to that in the earlier work.

While the global fits in Fig. 1 incorporate the charm production cross sections from HERA [13], they do not include the earlier charm structure function data from EMC [12]. Since the HERA cross sections are predominantly measured at small x, they have less sensitivity to the presence of IC than the fixed-target data at larger x, as the χ^2 profile in Fig. 1 illustrates. On the other hand, the EMC F_2^c measurements include data points at large x values, which do have greater impact on the IC determination. In Fig. 2(b) the χ^2 values for the global fits including the EMC data indicate a slight preference for a nonzero IC, with the EMC data alone favoring a value $\sim$(0.3–0.4)% (the additional threshold suppression factor has a minor impact on the EMC data). However, the description of the EMC data is clearly far from satisfactory, giving a χ^2 value of 4.3 per datum for 19 data points.

The comparison with the full set of F_2^c data from EMC is shown in Fig. 3 for several models of IC from Refs. [10,11], as well as for a fit without IC. At small x values ($x \lesssim 0.02$) the global fits generally overestimate the data, regardless of whether IC (which is negligible in this region) is included or not. At intermediate x ($0.02 \lesssim x \lesssim 0.1$), where the IC contributions are still small, the agreement improves, while at the largest x values ($x \gtrsim 0.2$) the fit with no IC clearly lies below the data. Here the addition of IC improves the agreement for all models considered, with the meson-baryon model for the confining c quark-diquark interaction [10] and the BHPS model [11] resulting in the biggest enhancement. On the other hand, the experimental uncertainties at the high x values are rather large compared with those in the small-x region, where the fit to the EMC F_2^c data is worse. Better agreement with the EMC data would require significantly larger IC at high x, together with some additional suppression mechanism at low x values, neither of which appear very probable. Because of the significant tension with the other global data sets, the EMC data are usually not included in most global PDF analyses [21–24,26–28,34].

These conclusions are more consistent with those reached in the MSTW analysis [34], which found reasonable fits including the EMC data for $N_{\rm IC} = 0.3\%$ using the BHPS model. On the other hand, the analysis [34] also utilized more stringent cuts ($Q^2 \geq 2$ GeV^2 and $W^2 \geq 15$ GeV^2) than those used in our fit, which removed much of the SLAC data at large x, and did not consider higher twist corrections—both of which are important in the region where IC is expected to contribute.

In summary, we have performed a comprehensive global QCD analysis of the world's high-energy scattering data, synthesizing the latest developments in global fitting technology and nonperturbative studies of charm production to fully exploit all of the available data that may have bearing on the question of IC in the nucleon. By relaxing the cuts on Q^2 and W^2 used in earlier global fits [20,22,34], while systematically accounting for finite-Q^2 and other hadronic and nuclear corrections [24,26,28], we found that the low-Q^2, high-x data from fixed-target experiments, in particular, place stronger constraints on the magnitude of IC than found previously. Excluding the older F_2^c measurements from the EMC [12], which give a very large χ^2, our fits generally rule out large values of IC, with $\langle x\rangle_{\rm IC}$ at most 0.5% at the 4σ level, even after taking into account nonperturbative charm threshold suppression factors. The tension between the EMC data and the more precise measurements of F_2^c at HERA at low x [13] has prompted many global PDFs analyses to omit these data from their fits. Given that the signal for IC relies so heavily on charm production data at large values of x, it would be essential to obtain new, more precise data on F_2^c to determine limits (upper or lower) on the nonperturbative charm content of the nucleon with greater confidence. Such measurements could be feasible at a future electron-ion collider facility [36].

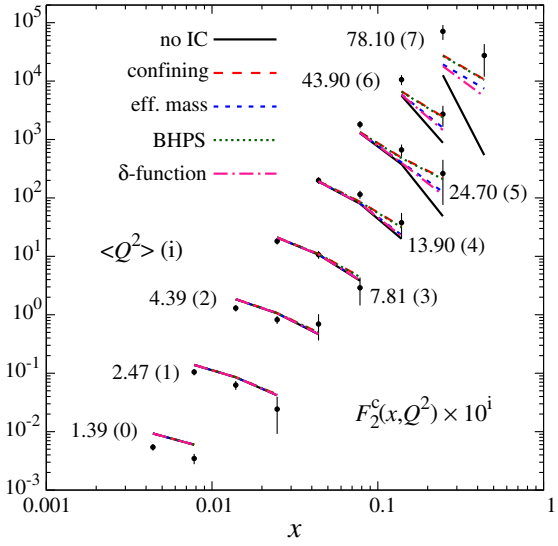

FIG. 3 (color online). Comparison of the total fitted F_2^c structure function with the full set of EMC data [12] for Q^2 between 1.39 to 78.1 GeV^2. The results with no IC (black solid lines) are compared with those using the confining (red dashed lines), effective mass (blue short-dashed lines), BHPS (green dotted lines), and δ-function (pink dot-dashed lines) models for IC [10].

This material is based upon work supported by the National Science Foundation (T. J. H. and J. T. L.) under Grant No. PHY-1205019. The work of T. J. H. was also supported in part by DOE Grants No. DE-FG02-87ER40365 and No. DE-FG02-97ER-41014. P. J.-D. and W. M. were supported by the DOE Contract No. DE-AC05-06OR23177, under which Jefferson Science Associates, LLC operates Jefferson Lab.

[1] J. Speth and A. W. Thomas, Adv. Nucl. Phys. **24**, 83 (1998).
[2] S. Kumano, Phys. Rep. **303**, 183 (1998).
[3] R. Vogt, Prog. Part. Nucl. Phys. **45**, S105 (2000).
[4] G. T. Garvey and J.-C. Peng, Prog. Part. Nucl. Phys. **47**, 203 (2001).
[5] W.-C. Chang and J.-C. Peng, Phys. Rev. Lett. **106**, 252002 (2011).
[6] J.-C. Peng and J.-W. Qiu, Prog. Part. Nucl. Phys. **76**, 43 (2014).
[7] P. Amaudruz *et al.*, Phys. Rev. Lett. **66**, 2712 (1991).
[8] E. A. Hawker *et al.*, Phys. Rev. Lett. **80**, 3715 (1998).
[9] D. Mason *et al.*, Phys. Rev. Lett. **99**, 192001 (2007).
[10] T. J. Hobbs, J. T. Londergan, and W. Melnitchouk, Phys. Rev. D **89**, 074008 (2014).
[11] S. J. Brodsky, P. Hoyer, C. Peterson, and N. Sakai, Phys. Lett. B **93**, 451 (1980).
[12] J. J. Aubert *et al.*, Nucl. Phys. **B213**, 31 (1983); Phys. Lett. **94B**, 96 (1980); Phys. Lett. **110B**, 73 (1982).
[13] H. Abramowicz *et al.*, Eur. Phys. J. C **73**, 2311 (2013).
[14] E. Hoffmann and R. Moore, Z. Phys. C **20**, 71 (1983).
[15] B. W. Harris, J. Smith, and R. Vogt, Nucl. Phys. **B461**, 181 (1996).
[16] F. M. Steffens, W. Melnitchouk, and A. W. Thomas, Eur. Phys. J. C **11**, 673 (1999).
[17] W. Melnitchouk and A. W. Thomas, Phys. Lett. B **414**, 134 (1997).
[18] F. S. Navarra, M. Nielsen, C. A. A. Nunes, and M. Teixeira, Phys. Rev. D **54**, 842 (1996); F. O. Durães, F. S. Navarra, and M. Nielsen, Phys. Lett. B **498**, 169 (2001).
[19] J. Pumplin, Phys. Rev. D **73**, 114015 (2006).
[20] J. Pumplin, H. L. Lai, and W.-K. Tung, Phys. Rev. D **75**, 054029 (2007).
[21] W. K. Tung, H. L. Lai, A. Belyaev, J. Pumplin, D. Stump, and C.-P. Yuan, J. High Energy Phys. 02 (2007) 053.
[22] S. Dulat, T.-J. Hou, J. Gao, J. Huston, J. Pumplin, C. Schmidt, D. Stump, and C.-P. Yuan, Phys. Rev. D **89**, 073004 (2014).
[23] J. Gao, M. Guzzi, J. Huston, H.-L. Lai, Z. Li, P. Nadolsky, J. Pumplin, D. Stump, and C.-P. Yuan, Phys. Rev. D **89**, 033009 (2014).
[24] P. Jimenez-Delgado and E. Reya, Phys. Rev. D **89**, 074049 (2014).
[25] L. W. Whitlow, E. M. Riordan, S. Dasu, S. Rock, and A. Bodek, Phys. Lett. B **282**, 475 (1992).
[26] S. Alekhin, J. Blümlein, S. Klein, and S.-O. Moch, Phys. Rev. D **81**, 014032 (2010).
[27] A. Accardi, W. Melnitchouk, J. F. Owens, M. E. Christy, C. E. Keppel, L. Zhu, and J. G. Morfín, Phys. Rev. D **84**, 014008 (2011).
[28] J. F. Owens, A. Accardi, and W. Melnitchouk, Phys. Rev. D **87**, 094012 (2013).
[29] F. M. Steffens, M. D. Brown, W. Melnitchouk, and S. Sanches, Phys. Rev. C **86**, 065208 (2012).
[30] D. de Florian and R. Sassot, Phys. Rev. D **69**, 074028 (2004).
[31] P. Jimenez-Delgado, Nucl. Phys. B, Proc. Suppl. **186**, 51 (2009).
[32] M. Arneodo *et al.*, Nucl. Phys. **B487**, 3 (1997).
[33] S. J. Brodsky, Conference presented at "HiX2014", Frascati, Italy (2014), http://www.lnf.infn.it/conference/HiX2014/.
[34] A. D. Martin, W. J. Stirling, R. S. Thorne, and G. Watt, Eur. Phys. J. C **63**, 189 (2009).
[35] P. Jimenez-Delgado, A. Accardi, and W. Melnitchouk, Phys. Rev. D **89**, 034025 (2014).
[36] A. Accardi *et al.*, arXiv:1212.1701.